Evaluation of Land Use/Land Cover Classification based on Different Bands of Sentinel-2 Satellite Imagery using Neural Networks

Mrs. Pallavi M[1]
Assistant Professor Dept. of CSE
Presidency University
Bangalore, India

Dr. Thivakaran T K[2]
Professor Dept. of CSE
Presidency University
Bangalore, India

Dr. Chandankeri Ganapathi[3]
Associate Professor, Dept. Name of Civil, Presidency University
Bangalore, India

***Abstract*—Spatial data analytics is an emerging technology. Artificial neural network techniques play a major role in analysing any critical dataset. Integrating remote sensing data with deep neural networks has led a way to several research problems. This paper aims at producing land use land cover map of Bangalore region, Karnataka, India with various band combinations of sentinel satellite imagery obtained from google earth engine. LULC map classes include water, urban, forest, vegetation and openland. Band combinations of satellite images represent different characteristics of spatial data. Hence, several band combinations are used to build LULC maps. Also, classified maps are generated using different neural networks with pixel-based classification approach. Appropriate performance metrics were identified to evaluate the classification results such as Accuracy, Precision, Recall, F1-score and Confusion Matrix. Among neural networks, Convolutional Neural Network technique outperformed with 98.1 % of accuracy and less error rates in confusion matrix considering RGBNIR (4328) band combination of satellite imagery.**

Keywords*—Sentinel-2; neural networks; convolutional neural networks; remote sensing data; land use land cover maps

I. Introduction

Monitoring the Earth's surface has undergone a radical change as a result of advances in satellite remote sensing technology. Sentinel-2 multispectral products, created as a result of the European Space Agency's (ESA) [2] and European Union's (EU) [3] Copernicus Programme, have helped to effectively monitor the Earth's surface [1]. The ESA Sentinel-2 satellite constellation, which includes multispectral scanners on board [35], is the second iteration of the Sentinel satellite programme. Sentinel-2's main goal is to supply high resolution [33] satellite data for observing changes in climate [34], monitoring natural disasters, and tracking changes in land cover and use. It also aims to supplement previous satellite missions like Landsat.

Sentinel level-2A dataset acquired is of one of the metropolitan cities of India i.e., Bangalore which was obtained from Google earth engine. A wide-swath, high-resolution, multi-spectral [2] imaging mission from Europe is called SENTINEL-2. The twin satellites' complete mission specification calls for a high return frequency of five days [33] at the equator when they are in the same orbit but phased at 180°. With a spatial resolution of four bands at 10 m, six bands at 20 m, and three bands at 60 m, the optical payload on SENTINEL-2 will sample thirteen spectral bands [34]. It is possible to use the 290 km-wide orbital sweep. Based on Level-1C data with atmospheric correction for reflectance from the Bottom of the Atmosphere (BoA), data are used to create the Level-2A product [3]. They are routinely manufactured by ESA as of January 2019, exactly like the level 1C products previously mentioned.

The open access Sen2Cor processor allows users to continue producing their own BoA data from Level 1C. Water vapour map [35], Aerosols optical thickness map and a basic scene classification map [2] are among the extra Sen2Cor algorithm outputs that are included in Level 2A data. Sentinel Satellite Image Time Series (SITS) [3] have recently been productively utilised in the perspective of LULC mapping, illuminating the advantages of having access to such optical and radar SITS in this field. A few noteworthy examples include the creation of country-scale land cover maps using optical Sentinel SITS [4].

The following Table I shows the important features of Sentinel level-2 image.

The ideas of LULC laid the foundation to understand how people interact with the environment [6]. The term "Land Use" describes the purposes for which humans use the land cover, such as anthropogenic activity-induced changes. The term "land cover" describes the natural elements [5] that make up the surface of the Earth, such as agricultural land, aquatic sources, and topsoil. [7].

As deep learning techniques automate feature extraction and classification, it is more suitable and efficient for satellite imagery [8]. Each layer of deep learning model computes new data pattern from previous layers' data understanding of artificial neurons, resulting in order of data generalisations [9]. Convolution [32] and pooling layers [31] are typically followed by a fully connected neural network layer [19] and a suitable activation function [37] in CNNs, finally corresponding LULC class is predicted by softmax function as an output [10].

TABLE I. SENTINEL LEVEL-2 IMAGERY'S CHARACTERISTICS [3]

Spatial Resolution	Band Number	Central Wavelength (nm)	Bandwidth (nm)	Lref (reference radiance) (W m -2 sr-1 µm-1)	SNR @ Lref
10m	2	490	65	128	154
	3	560	35	128	168
	4	665	30	108	142
	8	842	115	103	172
20m	5	705	15	74.5	117
	6	740	15	68	89
	7	783	20	67	105
	8b	865	20	52.5	72
	11	1610	90	4	100
	12	2190	180	1.5	100
60m	1	443	20	129	129
	9	945	20	9	114
	10	1375	30	6	50

A. Study Area

The great capital of the Indian Karnataka state, Bangalore [36] is one of the cities with the greatest population growth. The most populated district in the state, accounting for 15.8% of the state's total population, is located in Karnataka's only metropolitan region, which has a total population of 96,21,551 (as of the 2011 census). The district's total area is 2196 sq. km, with 4381 people residing in each sq. km. In terms of both land and population, it is the largest district in the state of Karnataka. The majority of Bangalore's population lives in urban areas, making it the most urbanised district.

Bengaluru as showed in Fig. 1 is located on the Deccan Plateau [28], in the Karnataka state's south eastern part. The Bengaluru district lies between 120 58' to 13o 0' North Latitude and 770 37' to 78o 18' East Longitude. The district's elevation is typically about 1000m above the mean sea level which bestows it with a healthy climate. The district has four taluks namely Bengaluru North, South, East, and Anekal. The famous IT and BT Electronic City situated in Anekal taluk [36].

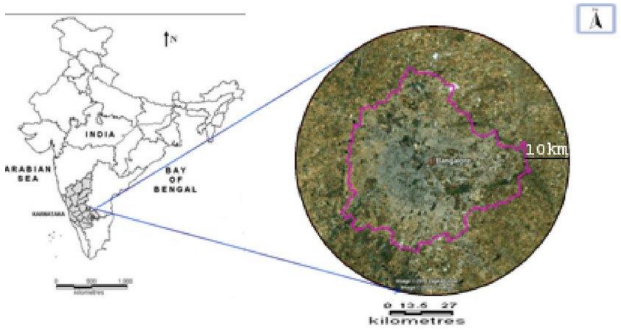

Fig. 1. Bangalore BBMP Limits Study Area [28].

II. RELATED WORK

Sentinel-2 image of Bangalore region was tiled into patches and for the identified land use land cover classes of trained patches, CNN architectures such as DenseNet201, VGG16 and Resnet50 were applied. This yielded better classification results. [27].

Quick Bird datasets of the regions Rome, Las Vegas and Florida were used for the scene classification using Support Vector machine's margin sampling approach and Entropy query by bagging which is a classifier independent method [13]. Kappa index was mainly used along with accuracy to evaluate the pixel based classification in this study.

Four classes (Water, Cropland, Forest and built-up) of LULC generated for the region Mandya, Karnataka using five bands of Sentinel-2A namely SWIT, NIR, Blue, Red and Green with F1-Score of 0.84 using modified Segnet architecture of deep learning [11].

High resolution image datasets of urban areas of China, Italy and Germany were used with Deep Convolutional neural network techniques for the classification of land use and achieved accuracies of about 90% using object-based and pixel-based approaches [12].

Sentinel 2 image bands of 4, 3, 2, 8 were used for the land cover classification of central java region of Indonesia. With the ArcMap tool and supervised classification approach, a very high accuracy of 1 and moderate kappa value of 0.4896 [14] were achieved. Maximum Likelihood classifier used in this research is then assessed by comparing raster values of classified image and actual google earth engine image. For this, acquisition dates of two images are kept same.

Maximum Likelihood Classifier (MLC) and Support Vector Machine (SVM) classifiers of ERDAS imagine tool were applied on Sentinel-2 and Landsat-8 dataset of Istanbul metropolitan city of Turkey's LULC classes [15]. Among these two classifiers, SVM achieved highest accuracy and kappa coefficient of 84.17% and 0.8190 respectively for the sentinel-2 data. Error matrix was calculated against classified random points and reference points of google earth also as an assessment.

Zonguldak, Turkey [16] was considered as the study area in this research. Sentinel -2 MSI and Landsat OLI were used as satellite imageries. MLC was used to generate LULC map. Classification using Sentinel-2 data yielded highest accuracy and kappa coefficient than Landsat-8. Accuracy was assessed with 460 stratified random points.

LULC maps and correlation matrix were generated for the Ahmedabad city of Gujarat state, India from the period 1991 to 2010 so as to know the change of certain land use classes. The main intension of this was to monitor population dynamics, urban expansion. [17].

This study presents application of LULC maps for the prediction of change and spatial distribution for the year 2027 of Ahmedabad city, Gujarat using the integration of cellular automata and artificial neural network model from temporal series of data from 1976 to 2017. [18].

Most of the recent research work focused on the LULC classification of satellite image patches (part of an image) of the interested areas. They were trained and fed to various neural, CNN architectures. But, LULC classification is required for the entire study area to perform change or any other spatial analysis. Only few GIS automated tools could do such classification for the entire study area rather than part of satellite image.

The main objective of this research is to generate optimal [29] land use land cover map using deep neural networks and convolutional neural networks approaches. In addition to this, various combinations of sentinel-2 image were evaluated to know the significance of each band. Finally, proposed model is evaluated using various metrics such as confusion matrix, precision, recall and F1-score. Model is validated with few randomly generated points which are then compared with google earth engine.

III. Methodology

The Fig. 2 process explains the data preparation before it is fed into the neural network. Firstly, Bangalore data is being extracted from sentinel portal through google earth engine using JavaScript. This requires date and year, proper selection of the region of interest, bands information. For the research we have downloaded, 2019's January till March data and used band combinations such as 843 (NIR, Red and Green), 432 (Red, Green, Blue) [14] and 8432 (NIR, Red, Green, Blue).

There are two important factors to select only Bruhat Bengaluru Mahanagara Palike (BBMP) limits within Bengaluru/Bangalore data. First, is to focus more on the urbanised areas so that change detection of LULC maps would be more interesting for further studies and second, is to reduce the study area image dimension so that computation time can also be lessened greatly. This phase is achieved by clipping only BBMP limits from whole Bangalore data.

As this research is done for medium spatial resolution image of 10m, pixel-based approach is more suitable [30]. Supervised classification approach is considered. For the same, training suites are generated based on the classes (Water, Urban, Forest, Vegetation and Open land). These suites are divided into train and test for the model evaluation. They are normalised within a scale of 255 so as to bring them into uniform range.

A. Neural Networks

The Fig. 3 shows the schematic representation of neural networks made use in the current work.

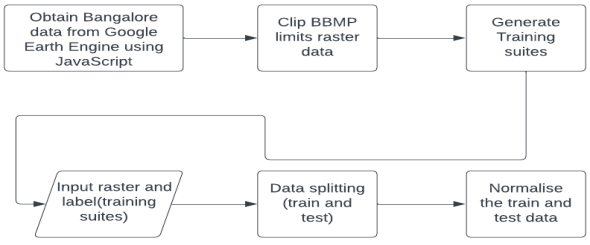

Fig. 2. Data Preparation Process.

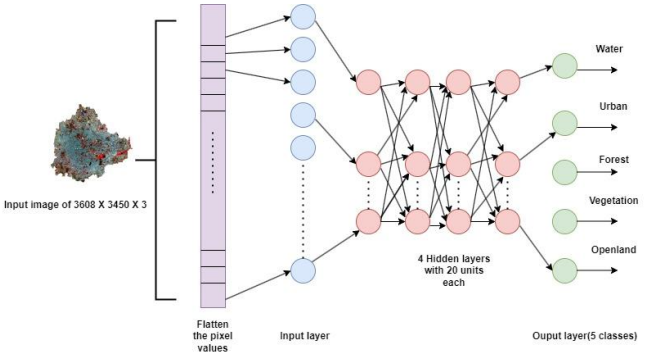

Fig. 3. Proposed Model of Deep Neural Networks.

Deep Neural Networks (DNN) are most efficiently used for multi-class classification [21]. As indicated in the above figure, we have used six layers in our proposed model. Firstly, input image is fed into the network. To ease the task, we have considered 80% of the input image pixels known as trained data out of the entire image. Pixel values are flattened and they are fed as neurons to the input layer. At hidden layer, sum of these inputs along with weights and bias as shown in equation (1) [19] is computed.

Relu activation function is applied to this sum as shown in equation (2) to activate neurons so that vanishing gradient problem could be overcome to some extent [20]. In this case, neuron values less than zero never gets activated. Likewise, process is repeated at next three hidden layers producing 20 units at each layer. Final hidden layer is connected output layer, wherein softmax function as represented in equation (3) finds the final predicted LULC class out of five as mentioned in the above figure.

$$z=\sum_i^n w_i x_i + b \quad (1)$$

here, n is number of input pixels

$$\delta(z) = \frac{1}{1+e^{-[(\sum_i^n w_i x_i)+b]}} \quad (2)$$

$$\sigma(z_i) = \frac{e^{z_i}}{\sum_{j=1}^k e^{z_i}} \quad (3)$$

here, k is 5 (number of classes).

Model's hyperparameters include learning rate of 0.001, 100 epochs, batch size of 128. Dropout of 20% and l2 regularisation are considered [38]. We have used keras library to implement this model in python.

B. Convolutional Neural Networks

The Fig. 4. shows the CNN model used in this work.

Convolutional, pooling, and affine layers combine to form Convolutional Neural Networks (CNN). When it comes to visual identification tasks, CNN's perform fantastically and at the cutting edge of technology [22]. CNN's are also used to classify remote sensing images with its extensive features. Here, we have used two layers of convolution and two pooling layers. Basically these layers are used to create feature maps of image size of 1247600 with three channels and 7X7 patch size [9]. Using a filter with a stack of fixed-size kernels (here, 5X5), the feature maps are produced at each layer of convolution and

passed into non-linearity using an activation function. The feature maps are then calculated as the weighted sum of the preceding layer of feature patches (e.g., ReLU) [32]. In this way, they maintain location invariance within the input data array while detecting local correlations (fitted in the kernel size) [37].

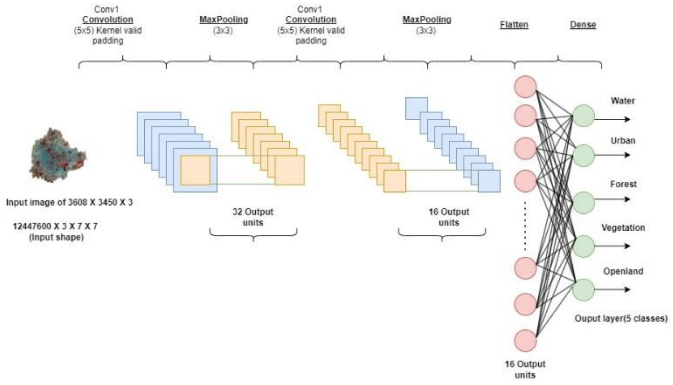

Fig. 4. Proposed Convolutional Neural Network Model.

By computing the maximum or average of nearby units to produce invariance to scaling, minor shifts, and distortions, the pooling layer (3X3) is utilised to minimise the dimension of the resulting feature map. A fully connected neural network and an activation function eventually complete the phases of convolution and pooling layers (32 and 16 units in first and second stage respectively), taking over control of the network's classification phase of five classes as described in the figure by further modeling non-linear relationships [23] of input features.

To train the model and to optimise the input features learnt, we have utilised learning rate of 0.001, epochs of 100, batch size of 128, loss function as Categorical Cross Entropy and Adam as optimiser [38]. The implementation was carried out using Pytorch for its robustness and Speed. Of course, high end system with GPU support was used for the research.

IV. Results and Discussion

In this section, firstly we have explained the results obtained using neural networks and then convolutional neural networks. For both the methodologies used in this study, BBMP region's sentinel level2 image of the period January to March 2020 data is fed as an input. Corresponding Predicted LULC maps are listed from Fig. 5-10. To create typical LULC map as in Geographical Information Systems (GIS), we have added latitude, longitude, scale bar, text, north arrow [26] to the classified image.

Error matrix is tabulated for all the five LULC classes i.e., Water, Urban, Forest, Vegetation and Openland for both DNN and CNN methods in terms of pixels. To compute this, only test data (20% of 12447600 pixels i.e., 2489520) obtained from the input as depicted in Fig. 2. is considered. Table II to IV and Table V to VII are the error matrices of DNN and CNN respectively.

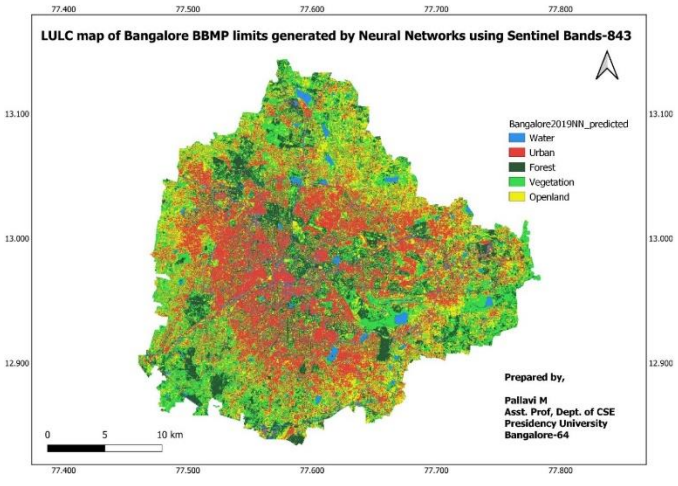

Fig. 5. LULC Classification Map Generated using Deep Neural Networks of the Sentinel Image Band Combination-843.

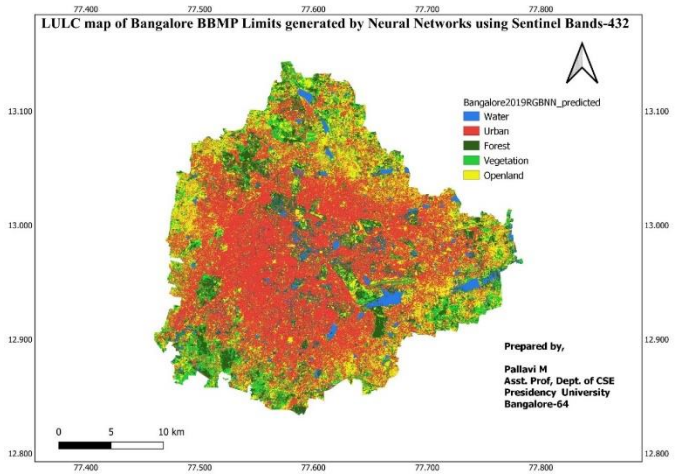

Fig. 6. LULC Classification Map Generated using Deep Neural Networks of the Sentinel Image Band Combination-432.

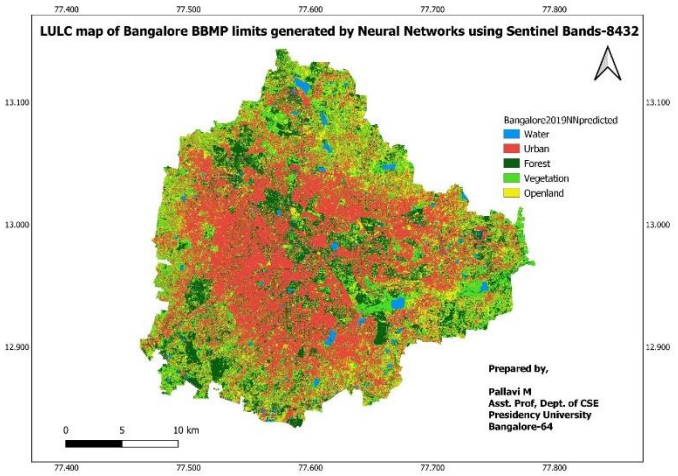

Fig. 7. LULC Classification Map Generated using Deep Neural Networks of the Sentinel Image Band Combination-8432.

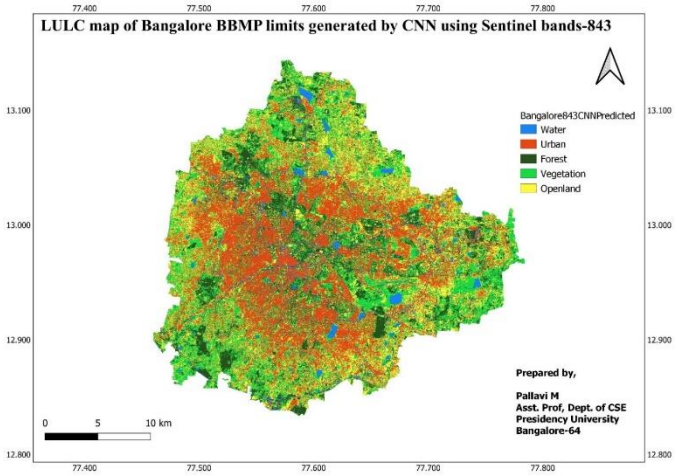

Fig. 8. LULC Classification Map Generated using Convolutional Neural Networks of the Sentinel Image Band Combination-843.

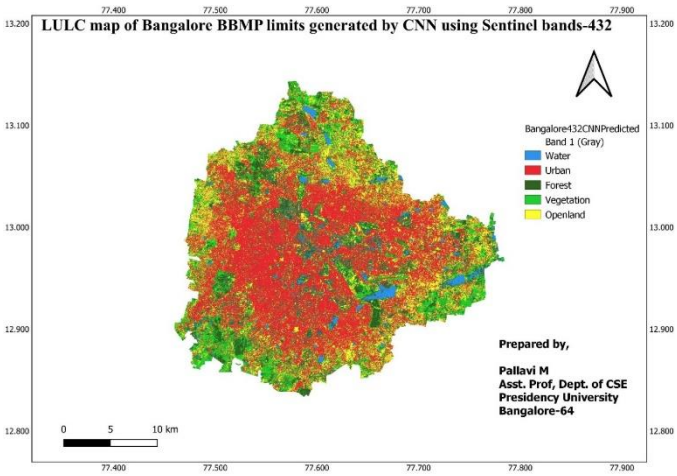

Fig. 9. LULC Classification Map Generated using Convolutional Neural Networks of the Sentinel Image Band Combination-432.

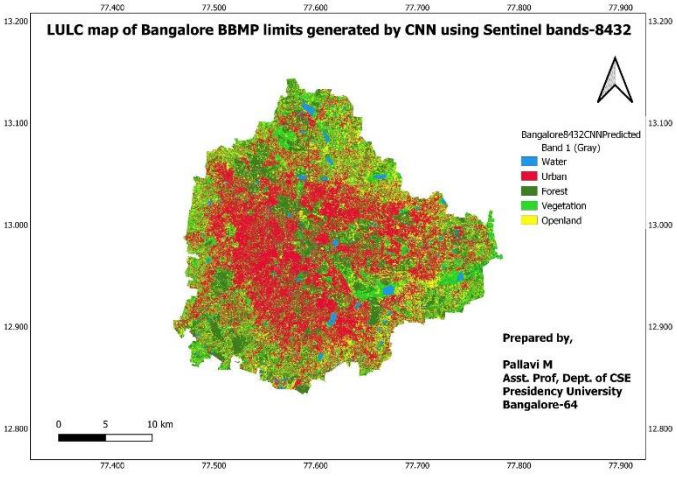

Fig. 10. LULC Classification Map Generated using Convolutional Neural Networks of the Sentinel Image Band Combination-8432.

TABLE II. CONFUSION MATRIX OBTAINED PER CLASS FOR THE TEST DATA USING DEEP NEURAL NETWORKS OF THE SENTINEL IMAGE BAND COMBINATION-843

	Water	Urban	Forest	Vegetation	Openland
Water	62599	517	3208	0	0
Urban	48	413647	729	2111	14688
Forest	2028	0	215668	3064	0
Vegetation	0	304	2419	373329	65736
Open land	0	14248	0	14353	277213

TABLE III. CONFUSION MATRIX OBTAINED PER CLASS FOR THE TEST DATA USING DEEP NEURAL NETWORKS OF THE SENTINEL IMAGE BAND COMBINATION-432

	Water	Urban	Forest	Vegetation	Openland
Water	53054	1271	9012	286	6
Urban	6703	624717	1567	21347	59603
Forest	13225	493	135680	10624	0
Vegetation	41	13464	41	188182	29
Open land	12	42483	0	18721	265349

TABLE IV. CONFUSION MATRIX OBTAINED PER CLASS FOR THE TEST DATA USING DEEP NEURAL NETWORKS OF THE SENTINEL IMAGE BAND COMBINATION-8432

	Water	Urban	Forest	Vegetation	Openland
Water	33210	2062	780	0	0
Urban	975	538202	109	15174	38255
Forest	2768	13	261038	1925	0
Vegetation	0	4306	1926	256390	41863
Open land	1386	14162	8522	31969	210875

TABLE V. CONFUSION MATRIX OBTAINED PER CLASS FOR THE TEST DATA USING CONVOLUTIONAL NEURAL NETWORKS OF THE SENTINEL IMAGE BAND COMBINATION-843

	Water	Urban	Forest	Vegetation	Openland
Water	57826	4237	2610	0	0
Urban	17	417627	2	66	11004
Forest	666	897	207906	12550	0
Vegetation	0	2150	107	373032	17568
Open land	0	7018	0	20414	330205

TABLE VI. CONFUSION MATRIX OBTAINED PER CLASS FOR THE TEST DATA USING CONVOLUTIONAL NEURAL NETWORKS OF THE SENTINEL IMAGE BAND COMBINATION-432

	Water	Urban	Forest	Vegetation	Openland
Water	52002	8033	12427	571	0
Urban	240	624769	3944	30624	22850
Forest	889	8	145358	39	0
Vegetation	1	397	6058	230483	2219
Open land	12	48162	0	21805	255008

TABLE VII. CONFUSION MATRIX OBTAINED PER CLASS FOR THE TEST DATA USING CONVOLUTIONAL NEURAL NETWORKS OF THE SENTINEL IMAGE BAND COMBINATION-8432

	Water	Urban	Forest	Vegetation	Openland
Water	35440	1761	878	0	257
Urban	361	549226	9	6823	2326
Forest	1056	134	259067	5990	6120
Vegetation	0	944	26	301016	3472
Open land	5	9231	95	7331	274330

The equations (4) - (6) are used for model evaluation metrics calculation, where m stands for number of classes (m=5) [24]

$$\text{Accuracy} = \frac{TP_m + TN_m}{TP_m + TN_m + FP_m + FN_m} \quad (4)$$

$$\text{Precision} = \frac{TP_m}{TP_m + FP_m} \quad (5)$$

$$\text{Recall} = \frac{TP_m}{TP_m + FN_m} \quad (6)$$

The Table VIII shows the overall Accuracy, P-Score and R-Score [25] of the DNN model for the test data. Among three different bands used, RGNIR-438 combination yielded the highest score.

The Table IX shows the overall Accuracy, P-Score and R-Score of the CNN model for the test data. Among three different bands used, RGBNIR-4328 combination yielded the highest score.

Fig. 11-16. to depict the Accuracy and loss graph of the DNN model for all the three band combinations used in this study.

TABLE VIII. CLASSIFICATION REPORT OF TEST DATA USING DEEP NEURAL NETWORKS OF VARIOUS SENTINEL BAND COMBINATIONS

Band Combination	Accuracy	P-Score	R-Score
RGNIR-438	95.04	0.950	0.950
RGB-432	92.00	0.920	0.920
RGBNIR-4328	93.32	0.933	0.933

TABLE IX. CLASSIFICATION REPORT OF TEST DATA USING CONVOLUTIONAL NEURAL NETWORKS OF VARIOUS SENTINEL BAND COMBINATIONS

Band Combination	Accuracy	P-Score	R-Score
RGNIR-438	96.8	0.968	0.968
RGB-432	93.6	0.936	0.936
RGBNIR-4328	98.1	0.981	0.981

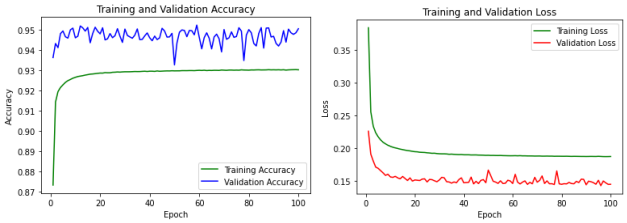

Fig. 11. Graph of Accuracy and Loss of Training and Validation Data using Deep Neural Networks of the Sentinel Image Band Combination-843.

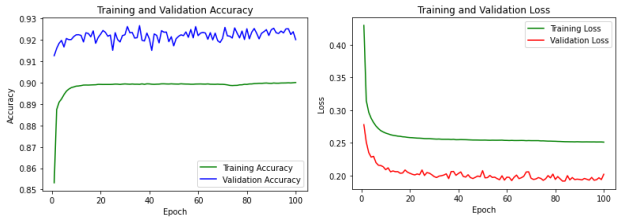

Fig. 12. Graph of Accuracy and Loss of Training and Validation Data using Deep Neural Networks of the Sentinel Image Band Combination-432.

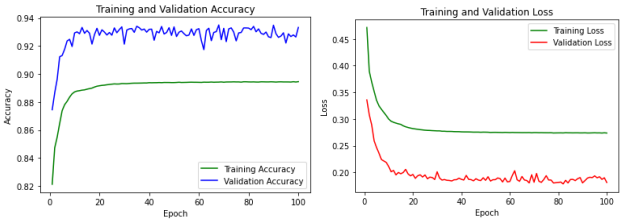

Fig. 13. Graph of Accuracy and Loss of Training and Validation Data using Deep Neural Networks of the Sentinel Image Band Combination-8432.

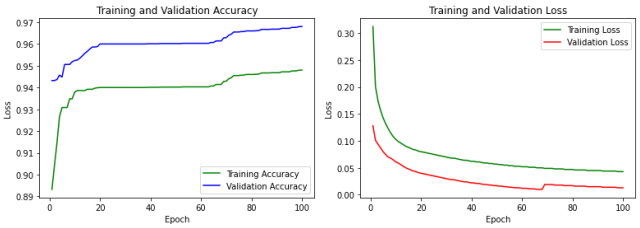

Fig. 14. Graph of Accuracy and Loss of Training and Validation Data using Convolutional Neural Networks of the Sentinel Image Band Combination-843.

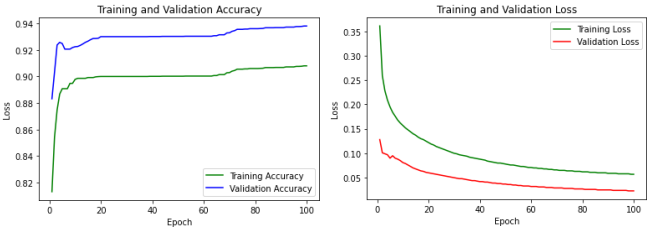

Fig. 15. Graph of Accuracy and Loss of Training and Validation Data using Convolutional Neural Networks of the Sentinel Image Band Combination-432.

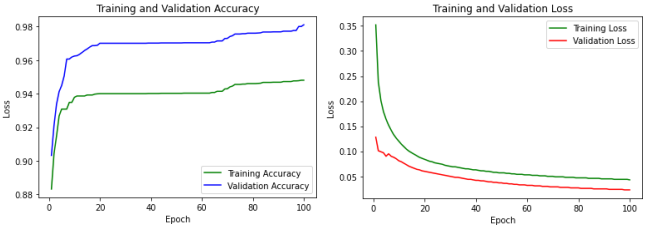

Fig. 16. Graph of Accuracy and Loss of Training and Validation Data using Convolutional Neural Networks of the Sentinel Image Band Combination-8432.

In addition to above results, CNN predicted LULC map of band combination RGBNIR is validated. This was done by generating 50 random points in the predicted image 10 for each class, then it was manually classified using google satellite

imagery. This classification was compared with the predicted image and error matrix for the same is as shown in Table X:

TABLE X. ERROR MATRIX GENERATED AGAINST 10 RANDOM POINTS FOR EACH CLASS WHICH ARE MANUALLY CLASSIFIED WITH GOOGLE SATELLITE IMAGE AGAINST PREDICTED CNN LULC MAP

	Classified (CNN Prediction)	**Water**	**Urban**	**Forest**	**Vegetation**	**Openland**	**Total**
Reference (10 Random points for validation)	**Water**	10	0	0	0	0	10
	Urban	0	8	0	0	2	10
	Forest	0	0	7	3	0	10
	Vegetation	0	1	2	7	0	10
	Openland	0	1	0	1	8	10

V. CONCLUSION

This study was conducted to examine the LULC maps obtained from neural networks techniques. The main objective was to determine the best suited neural network algorithm and the corresponding band combination with the highest accuracy, precision, recall and less error rate in the confusion matrix. To test all these, we chose Bangalore BBMP limits as the input image to the network and obtained land use and land cover of the typical classes Water, Urban, Forest, Vegetation and Openland. Among CNN and DNN and the sentinel-2 image band combinations RGB, RGBNIR and RGNIR, CNN with RGBNIR outperformed with accuracy 98.1 with less error rates in confusion matrix. Also, LULC map generated by the highest accuracy model (CNN with RGBNIR combination) was assessed with the help of google satellite imagery and confusion matrix was computed where in, error rate was very less.

LULC laid the foundation for further analysis. Mainly, change analysis will be performed and the predictive model would be developed in the upcoming research work mainly applications of LULC.

ACKNOWLEDGMENT

I would like to thank Dean Research and Innovation, Presidency University, Bangalore for providing high end systems to complete the second phase of my research as per the above mentioned results.

Conflicts of interest

The authors have no conflicts of interest to declare

REFERENCES

[1] Phiri, Darius, Matamyo Simwanda, Serajis Salekin, Vincent R. Nyirenda, Yuji Murayama, and Manjula Ranagalage. "Sentinel-2 data for land cover/use mapping: a review." Remote Sensing 12, no. 14 (2020): 2291.

[2] Szantoi, Zoltan, and Peter Strobl. "Copernicus Sentinel-2 calibration and validation." European Journal of Remote Sensing 52, no. 1 (2019): 253-255.

[3] ESA (European Space Agency). 2015a. “Sentinel-2 User Handbook, Issue 1, Rev 2, Revision 2.” ESA Standard Document. Accessed July 24 2015, 64 pages.

[4] Ienco, Dino, Roberto Interdonato, Raffaele Gaetano, and Dinh Ho Tong Minh. "Combining Sentinel-1 and Sentinel-2 Satellite Image Time Series for land cover mapping via a multi-source deep learning architecture." ISPRS Journal of Photogrammetry and Remote Sensing 158 (2019): 11-22.

[5] ED Chaves, Michel, Michelle CA Picoli, and Ieda D. Sanches. "Recent applications of Landsat 8/OLI and Sentinel-2/MSI for land use and land cover mapping: A systematic review." Remote Sensing 12, no. 18 (2020): 3062.

[6] Gómez, Cristina, Joanne C. White, and Michael A. Wulder. "Optical remotely sensed time series data for land cover classification: A review." ISPRS Journal of Photogrammetry and Remote Sensing 116 (2016): 55-72.

[7] Lambin, Eric FMDA, Mark DA Rounsevell, and Helmut J. Geist. "Are agricultural land-use models able to predict changes in land-use intensity?." Agriculture, Ecosystems & Environment 82, no. 1-3 (2000): 321-331.

[8] Vaishnnave, M. P., K. Suganya Devi, and P. Srinivasan. "A study on deep learning models for satellite imagery." International Journal of Applied Engineering Research 14, no. 4 (2019): 881-887.

[9] Vali, Ava, Sara Comai, and Matteo Matteucci. "Deep learning for land use and land cover classification based on hyperspectral and multispectral earth observation data: A review." Remote Sensing 12, no. 15 (2020): 2495.

[10] LeCun, Yann, Yoshua Bengio, and Geoffrey Hinton. "Deep learning." nature 521, no. 7553 (2015): 436-444.

[11] Sathyanarayanan, Dinesh, D. V. Anudeep, C. Anjana Keshav Das, Sanat Bhanadarkar, D. Uma, R. Hebbar, and K. Ganesha Raj. "A Multiclass Deep Learning Approach for LULC Classification of Multispectral Satellite Images." In 2020 IEEE India Geoscience and Remote Sensing Symposium (InGARSS), pp. 102-105. IEEE, 2020.

[12] Zhao, Wenzhi, Shihong Du, and William J. Emery. "Object-based convolutional neural network for high-resolution imagery classification." IEEE Journal of Selected Topics in Applied Earth Observations and Remote Sensing 10, no. 7 (2017): 3386-3396.

[13] Tuia, Devis, Frédéric Ratle, Fabio Pacifici, Mikhail F. Kanevski, and William J. Emery. "Active learning methods for remote sensing image classification." IEEE Transactions on Geoscience and Remote Sensing 47, no. 7 (2009): 2218-2232.

[14] Miranda, Eka, Achmad Benny Mutiara, and Wahvu Catur Wibowo. "Classification of land cover from Sentinel-2 imagery using supervised classification technique (preliminary study)." In 2018 International Conference on Information Management and Technology (ICIMTech), pp. 69-74. IEEE, 2018.

[15] Topaloğlu, Raziye Hale, Elif Sertel, and Nebiye Musaoğlu. "Assessment of Classification Accuracies of Sentinel-2 And Landsat-8 Data for Land Cover/Use Mapping." International archives of the photogrammetry, remote sensing & spatial Information Sciences 41 (2016).

[16] Sekertekin, A., A. M. Marangoz, and H. Akcin. "Pixel-based classification analysis of land use land cover using Sentinel-2 and Landsat-8 data." Int. Arch. Photogramm. Remote Sens. Spat. Inf. Sci 42 (2017): 91-93.

[17] Sikarwar, Ankit, and Aparajita Chattopadhyay. "Change in land use-land cover and population dynamics: A town-level Study of Ahmedabad city sub-District of Gujarat." International Journal of Geomatics and Geosciences 7, no. 2 (2016): 225-234.

[18] Yatoo, Saleem Ahmad, Paulami Sahu, Manik H. Kalubarme, and Bhagirath B. Kansara. "Monitoring land use changes and its future prospects using cellular automata simulation and artificial neural network for Ahmedabad city, India." GeoJournal (2020): 1-22.

[19] Németh, Gergely Dániel, and Judit Ács. "Hyphenation using deep neural networks." V. Vincze (szerk.) XIV. Magyar Számítógépes Nyelvészeti Konferencia (MSZNY 2018) (2018): 146-158.

[20] Jin, Jing, Feng, Wei Zhang, Jianan Zhang, Zhihao Zhao, and Qi-Jun Zhang. "Recent advances in deep neural network technique for high-dimensional microwave modeling." In 2020 IEEE MTT-S International Conference on Numerical Electromagnetic and Multiphysics Modeling and Optimization (NEMO), pp. 1-3. IEEE, 2020.

[21] Tahir, Waleed, Aamir Majeed, and Tauseef Rehman. "Indoor/outdoor image classification using gist image features and neural network classifiers." In 2015 12th International Conference on High-Capacity

Optical Networks and Enabling/Emerging Technologies (HONET), pp. 1-5. IEEE, 2015.

[22] Tiwari, Vaibhav, Chandrasen Pandey, Ankita Dwivedi, and Vrinda Yadav. "Image classification using deep neural network." In 2020 2nd International Conference on Advances in Computing, Communication Control and Networking (ICACCCN), pp. 730-733. IEEE, 2020.

[23] Emmert-Streib, Frank, Zhen Yang, Han Feng, Shailesh Tripathi, and Matthias Dehmer. "An introductory review of deep learning for prediction models with big data." Frontiers in Artificial Intelligence 3 (2020): 4.

[24] Grandini, Margherita, Enrico Bagli, and Giorgio Visani. "Metrics for multi-class classification: an overview." arXiv preprint arXiv:2008.05756 (2020).

[25] Alejo, Roberto, J. A. Antonio, Rosa Maria Valdovinos, and J. Horacio Pacheco-Sánchez. "Assessments metrics for multi-class imbalance learning: A preliminary study." In Mexican Conference on Pattern Recognition, pp. 335-343. Springer, Berlin, Heidelberg, 2013.

[26] Krygier, John, and Denis Wood. Making maps: a visual guide to map design for GIS. Guilford Publications, 2016.

[27] Pallavi, M., T. K. Thivakaran, and Chandankeri Ganapathi. "A Tile-Based Approach for the LULC Classification of Sentinel Image Using Deep Learning Techniques." In 2022 International Conference for Advancement in Technology (ICONAT), pp. 1-5. IEEE, 2022.

[28] Setturu, Bharath, Uttam Kumar, and T. V. Ramachandra. "Spatio-Temporal Pattern of Landuse Dynamics for Bangalore, 2010".

[29] Pallavi M, T. K. Thivakaran, and Chandankeri Ganapathi. "A Land Use Land Cover Map Generation Of Satellite Image Using Deep Learning Techniques.". Indian Journal of Computer Science and Engineering (IJCSE), Vol. 13 No. 4 Jul-Aug 2022, DOI: 10.21817/indjcse/2022/v13i4/221304027.

[30] Duro, Dennis C., Steven E. Franklin, and Monique G. Dubé. "A comparison of pixel-based and object-based image analysis with selected machine learning algorithms for the classification of agricultural landscapes using SPOT-5 HRG imagery." Remote sensing of environment 118 (2012): 259-272.

[31] Arora, Divya, Mehak Garg, and Megha Gupta. "Diving deep in deep convolutional neural network." In 2020 2nd International Conference on Advances in Computing, Communication Control and Networking (ICACCCN), pp. 749-751. IEEE, 2020.

[32] Pomerat, John, Aviv Segev, and Rituparna Datta. "On neural network activation functions and optimizers in relation to polynomial regression." In 2019 IEEE International Conference on Big Data (Big Data), pp. 6183-6185. IEEE, 2019.

[33] Bousbih, Safa, Mehrez Zribi, Mohammad El Hajj, Nicolas Baghdadi, Zohra Lili Chabaane, Pascal Fanise, and Gilles Boulet. "Sentinel-1 and Sentinel-2 data for soil moisture and irrigation mapping over semi-arid region." In IGARSS 2019-2019 IEEE International Geoscience and Remote Sensing Symposium, pp. 7022-7025. IEEE, 2019.

[34] De Luca, Giandomenico, João MN Silva, Salvatore Di Fazio, and Giuseppe Modica. "Integrated use of Sentinel-1 and Sentinel-2 data and open-source machine learning algorithms for land cover mapping in a Mediterranean region." European Journal of Remote Sensing 55, no. 1 (2022): 52-70.

[35] Traganos, Dimosthenis, and Peter Reinartz. "Mapping Mediterranean seagrasses with Sentinel-2 imagery." Marine pollution bulletin 134 (2018): 197-209.

[36] Dittrich, Christoph. "Bangalore: Globalisation and fragmentation in India's hightech-capital." Asien 103, no. 3 (2007): 45-58.

[37] Ramprasath, Muthukrishnan, M. Vijay Anand, and Shanmugasundaram Hariharan. "Image classification using convolutional neural networks." International Journal of Pure and Applied Mathematics 119, no. 17 (2018): 1307-1319.

[38] Wang, Yifeng, Yang Wang, Hongyi Li, Zhuoxi Cai, Xiaohan Tang, and Yin Yang. "CNN Hyperparameter optimization based on CNN visualization and perception hash algorithm." In 2020 19th International Symposium on Distributed Computing and Applications for Business Engineering and Science (DCABES), pp. 78-82. IEEE, 2020.